

# Unraveling the chemical dynamics of bimolecular reactions of ground state boron atoms, $B(^2P_j)$ , with acetylene, $C_2H_2(X^1\Sigma_g^+)$

R. I. Kaiser,<sup>\*a</sup> N. Balucani,<sup>b</sup> N. Galland,<sup>c</sup> F. Caralp,<sup>c</sup> M. T. Rayez<sup>c</sup> and Y. Hannachi<sup>c</sup>

<sup>a</sup> Department of Chemistry, University of Hawaii, Honolulu HI 96822, USA.

E-mail: kaiser@gold.chem.hawaii.edu

<sup>b</sup> Dipartimento di Chimica, Università di Perugia, 06123 Perugia, Italy

<sup>c</sup> Laboratoire de Physico-Chimie Moléculaire (CNRS UMR 5803), Université Bordeaux I, 351, Cours de la Libération, 330405 Talence Cedex, France

Received 27th November 2003, Accepted 29th January 2004  
First published as an Advance Article on the web 8th March 2004

The reaction dynamics of atomic boron,  $B(^2P)$ , with acetylene,  $C_2H_2(X^1\Sigma_g^+)$ , were investigated at two collision energies of  $12.9 \text{ kJ mol}^{-1}$  and  $16.3 \text{ kJ mol}^{-1}$  employing the crossed molecular beams technique. Only the atomic boron *versus* hydrogen atom exchange pathway was observed. Forward-convolution fitting of the laboratory data at  $m/z = 36$  ( $^{11}BC_2H^+$ ) shows that the reaction dynamics are indirect, proceed *via* addition of the boron atom to the carbon-carbon triple bond *via* a cyclic intermediate, and form the linear  $HBCC(X^1\Sigma^+)$  molecule after an atomic hydrogen ejection. The formation of the  $HBCC(X^1\Sigma^+)$  isomer under single collision conditions presents the first “clean” gas phase synthesis of this important organo-boron molecule and opens the door to a prospective spectroscopic investigation.

## I. Introduction

Untangling the chemical dynamics of elementary reactions of atomic boron,  $B(^2P_j)$ , offers an important means to understand the role of boron particles in material sciences,<sup>1</sup> boron assisted nanotube growth,<sup>2</sup> high temperature combustion processes,<sup>3,4</sup> interstellar environments,<sup>5</sup> and fundamental reaction mechanisms involving organo-boron species.<sup>6,7</sup> For many years, the interest in boron ignition and combustion fueled extensive research to characterize the temperature profile of boron-based flames of high energy density materials.<sup>8–10</sup> Bimolecular boron reactions are also of potential importance to the chemical evolution of the interstellar medium. Here,  $^{11}B$  can be formed either in type II supernova explosions or in the interstellar medium through spallation reactions between cosmic ray particles and interstellar nuclei.<sup>11–13</sup> These processes support a boron abundance with fractions of about  $2.5 \times 10^{-10}$  relative to atomic hydrogen.<sup>14</sup>

Very recently, particular attention has been devoted to actually investigate elementary reactions of boron atoms with hydrocarbons *via* matrix isolation techniques<sup>15–18</sup> and under single collision conditions employing the crossed molecular beam technique.<sup>19–21</sup> These experiments gained a deeper insight in the formation of organo-boron molecules of the generic formula  $BC_xH_y$ , which are isoelectronic to the corresponding  $C_{x+1}H_y$  cations.<sup>22</sup> Andrews and coworkers utilized matrix trapping to identify various  $BC_2H_n$  ( $n = 1–5$ ) isomers *via* infrared spectroscopy after co-depositing laser ablated boron atoms with acetylene,<sup>15</sup> ethylene,<sup>16,17</sup> and ethane<sup>18</sup> in an argon matrix. However, the poorly defined distributions of atomic boron velocities and electronic spin states together with the effect of matrix trapping make it difficult to assign the reaction mechanisms unambiguously. On the other hand, an investigation at the molecular level, in a collision free environment, where it is possible to observe the consequences of a single reactive event, can provide a direct insight into the reaction micro-mechanism.<sup>23</sup> The crossed molecular beam method with mass spectrometric detection is particularly suitable for investigating reactions giving polyatomic products which are not

*a priori* predictable and/or whose spectroscopic properties are unknown (see for instance refs. 24 and 25). We have recently succeeded in generating a pulsed beam of boron atoms by laser ablation of a boron rod and undertaken a systematic study of  $B(^2P)$  reactions with simple unsaturated hydrocarbons of practical importance, such as ethylene<sup>19</sup> and benzene.<sup>20</sup> These studies presented detailed mechanisms on how the aromatic molecules with  $2\pi$  Hückel electrons, borirene, and  $6\pi$  Hückel electrons, benzoborirene, are formed *via* an initial addition of the boron atom to the unsaturated bond of the hydrocarbon molecule followed by isomerization and subsequent elimination of atomic hydrogen (Fig. 1). A preliminary account of the first experimental results on the reaction with acetylene at a collision energy of  $16.3 \text{ kJ mol}^{-1}$  has been given as well; in that first work a  $HBCC$  reaction product formed *via* an atomic boron *versus* hydrogen exchange pathway was identified.<sup>21</sup> Here, we report a comprehensive investigation on how the dynamics of the  $B/C_2H_2$  system and the underlying micro-channels vary with the collision energy and carry out also statistical RRKM calculations.

## II. Experiment and data analyses

The experiments were performed at two collision energies employing the 35" crossed molecular beam machine, which

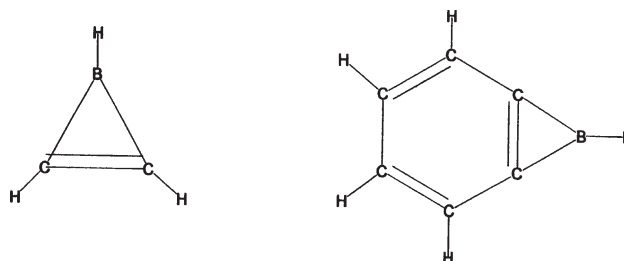


**Fig. 1** Structure of the borirene (left) and benzoborirene (right) molecules formed upon the reaction of atomic boron with ethylene and benzene, respectively, under single collision conditions.

has been described in detail elsewhere.<sup>24,26</sup> Briefly, the atomic boron beam was produced *via* laser ablation of a boron rod at 266 nm by employing the same experimental set-up described in ref. 27. The 30 Hz, 35–40 mJ output of a Spectra Physics GCR 270-30 Nd-YAG laser was focused on a rotating boron rod, and ablated atoms were seeded into helium gas which was released by a Proch-Trickl pulsed valve. A rotating chopper wheel was mounted after the ablation zone to select a 9  $\mu\text{s}$  segment of the pulse with peak velocities of  $1590 \pm 10 \text{ ms}^{-1}$  and  $1846 \pm 5 \text{ ms}^{-1}$  and speed ratios  $S$  of  $9.0 \pm 0.1$  and  $7.9 \pm 0.1$ , respectively for the two experiments. The  $\text{B}(^2\text{P})$  beams crossed a pulsed acetylene beam ( $v_p = 900 \pm 10 \text{ ms}^{-1}$ ,  $S = 9.0 \pm 0.1$ ) at  $90^\circ$  in the interaction region of the scattering chamber at averaged collision energies of  $E_c = 12.9 \pm 0.2 \text{ kJ mol}^{-1}$  and  $16.3 \pm 0.4 \text{ kJ mol}^{-1}$  in the interaction region. Note that natural boron has two isotopes of  $m/z = 11$  (80%) and 10 (20%), and the reported collision energies refer to the  $^{11}\text{B}$  isotope. The scattered species were monitored *via* time-of-flight (TOF) spectra using a triply differentially pumped ultra high vacuum ( $< 8 \times 10^{-15}$  mbar) detector consisting of a Brink-type electron impact ionizer, a quadrupole mass filter, and a Daly ion detector. To obtain information on the reaction dynamics, we have derived the best-fit center-of-mass (CM) functions from TOF spectra and laboratory angular distributions (LAB) by using a forward-convolution technique. In this iterative procedure trial CM angular,  $T(\theta)$ , and translational energy,  $P(E_T)$ , flux distributions (assumed to be independent of each other) are used until a best fit of the experimental distributions is achieved. This program also accounts for the machine as well as beam parameters (velocity spread, angular divergence). Both the functions  $T(\theta)$  and  $P(E_T)$  contain the basic information of the nature of scattering process and of the reaction micromechanism(s).<sup>24</sup>

### III. RRKM calculations

The microcanonical rate constants  $k(E)$  of important steps are obtained from the RRKM theory *via* the expression:

$$k(E) = G(E)/h \times N(E). \quad (1)$$

Here,  $E$  is the collision energy,  $h$  the Planck constant,  $G(E)$  the number of energetically accessible states at the transition state, and  $N(E)$  the density of states of the reactant species; the density of states was calculated with the help of G2 *ab initio* calculations.<sup>28</sup> All species are treated as symmetric tops; the external  $K$ -rotor, associated with the smallest moment of inertia is treated as an active degree of freedom completely coupled with vibrations. The density of states of the reactants species and the sum of states for the transition state are derived by taking the inverse Laplace transform of the corresponding partition functions<sup>29</sup> calculated with the structural parameters obtained from previous theoretical calculations.<sup>21</sup> The calculated microcanonical rate constants are reported in Table 1.

### IV. Experimental results

Reactive scattering signal was detected at both collision energies at mass to charge ratios  $m/z = 36$  ( $^{11}\text{BC}_2\text{H}^+$ ),  $m/z = 35$  ( $^{10}\text{BC}_2\text{H}^+ / ^{11}\text{BC}_2^+$ ), and  $m/z = 34$  ( $^{10}\text{BC}_2^+$ ). Mass-to-charge ratios higher than 36 were not observed. At each angle, the

**Table 1** Calculated micro-canonical rate constants ( $\text{s}^{-1}$ )

Collision energy	$k_{4/3}$	$k_{3/4}$	$k_{4/5}$	$k_{5/4}$	$k_{4/6}$
$16.3 \text{ kJ mol}^{-1}$	$1.93 \times 10^{12}$	$4.54 \times 10^{11}$	$4.3 \times 10^{10}$	$1.79 \times 10^{11}$	$1.7 \times 10^8$
$12.9 \text{ kJ mol}^{-1}$	$1.86 \times 10^{12}$	$4.40 \times 10^{11}$	$3.8 \times 10^{10}$	$1.68 \times 10^{11}$	$6.1 \times 10^7$

TOF spectra at  $m/z = 35$  and 34 could be fit with the same center-of-mass functions as those data obtained at  $m/z = 36$ . This strongly indicates that only a molecule with gross formula  $\text{BC}_2\text{H}$  is the reaction product in this range of masses. This species is formed *via* an atomic boron *versus* hydrogen exchange. Note that the molecular hydrogen loss, which would yield also the corresponding  $\text{BC}_2$  fragment, is closed at both collision energies.

All the final data were collected at  $m/z = 36$  due to the most favorable signal-to-noise ratio. In Fig. 2 the TOF spectra recorded at  $E_c = 12.9 \text{ kJ mol}^{-1}$  are reported. In Fig. 3 the LAB distributions at both collision energies are also shown. The laboratory angular distribution at the collision energy of  $16.3 \text{ kJ mol}^{-1}$  has already been reported in ref. 21 and it is shown again here to outline the collision energy dependent trends in the laboratory data and in the center-of-mass functions. Both LAB distributions are peaked around the center-of-mass angles ( $\theta_{\text{CM}} \approx 49.0^\circ$  and  $53.0^\circ$ , for the higher and lower collision energies, respectively), but depict higher intensities in the forward directions with respect to the boron beams, that is at the left of the CM angle. Moreover, the distributions are quite broad and extend for  $40^\circ$  and  $50^\circ$  in the scattering plane defined by the acetylene and the boron beam.

At both collision energies, the experimental data were fit using a single CM translational energy distribution and a single CM angular distribution (Fig. 4). In our experiments, best fit of the LAB distribution and TOF spectra was achieved with  $P(E_T)$ s extending to 35–60  $\text{kJ mol}^{-1}$ . In each case, the best fit  $P(E_T)$  peaks away from  $E_T = 0$  and shows a maximum between 10 and 15  $\text{kJ mol}^{-1}$ . This ‘off-zero’ peaking could indicate a small exit barrier involved in the atomic hydrogen loss from the decomposing  $\text{BC}_2\text{H}_2$  intermediate. We recall, in fact, that while a peaking at zero translation energy is always indicative of a barrier-less fragmentation of the intermediate, a reaction which is barrier-less in the exit channel may also be characterized by a  $P(E_T)$  peak far from  $E_T = 0$  due to dynamical effects. Finally, the best fit  $P(E_T)$ s extend up to a translational energy range of 34–52  $\text{kJ mol}^{-1}$  ( $E_c = 12.9 \text{ kJ mol}^{-1}$ ) and 37–62  $\text{kJ mol}^{-1}$  ( $E_c = 16.3 \text{ kJ mol}^{-1}$ ). If we subtract the collision energies from the high-energy cutoffs, the resulting reaction exoergicity is found to be  $31 \pm 10 \text{ kJ mol}^{-1}$ .

The center-of-mass angular distributions are of help to gain additional information on the underlying reaction dynamics. At both collision energies the product scattering intensity is distributed in the entire angular range from  $0^\circ$  to  $180^\circ$  pointing

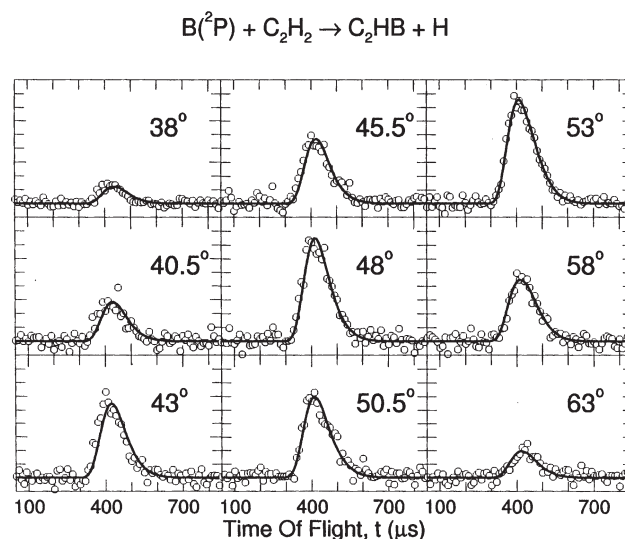


**Fig. 2** Selected time-of-flight spectra at  $m/z = 36$  at distinct laboratory angles recorded at a collision energy of  $12.9 \text{ kJ mol}^{-1}$ . The circles represent the experimental data, the solid lines the calculated fit.

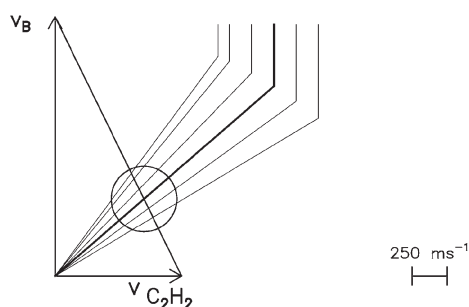
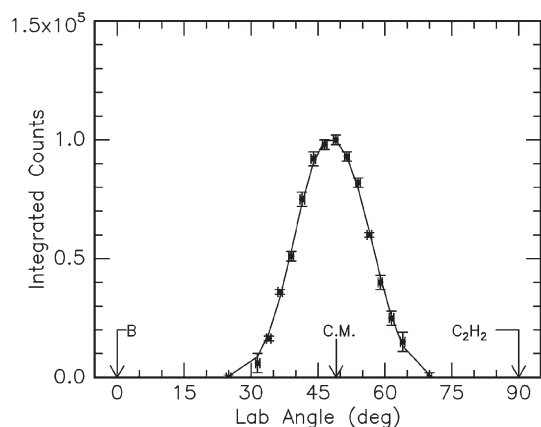
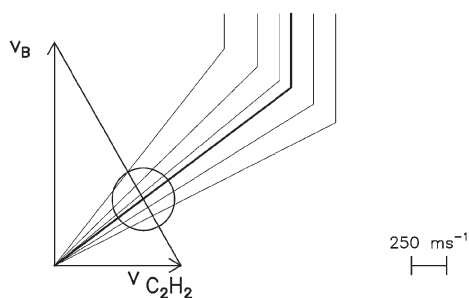
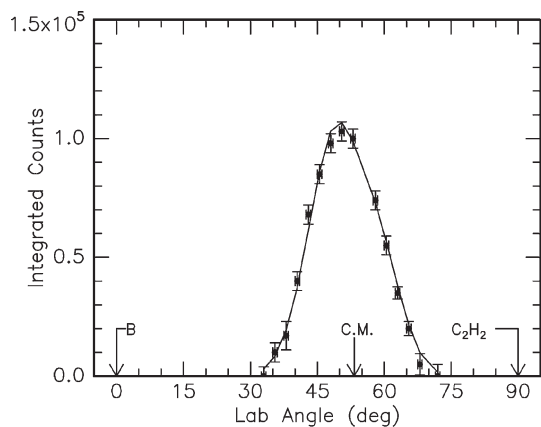


**Fig. 3** Laboratory angular distributions of the  $^{11}\text{BC}_2\text{H}$  product at  $m/z = 36$  at collision energies of  $12.9 \text{ kJ mol}^{-1}$  (top) and  $16.3 \text{ kJ mol}^{-1}$  (bottom) investigated for the  $\text{B}/\text{C}_2\text{H}_2$  system. Dots and error bars indicate experimental data, the solid lines the calculated distribution with the best-fit center-of-mass functions.

to the formation of  $\text{BC}_2\text{H}_2$  bound intermediate(s). A slight preference for forward scattering (with respect to the boron beam) is clearly visible in both cases. Interestingly, the preference for forward scattering decreases as the collision energy rises from  $12.9 \text{ kJ mol}^{-1}$  to  $16.3 \text{ kJ mol}^{-1}$ , with an intensity ratio of  $I(0^\circ)/I(180^\circ) = 1.65 \pm 0.05$  and  $1.20 \pm 0.05$  at the lower and higher

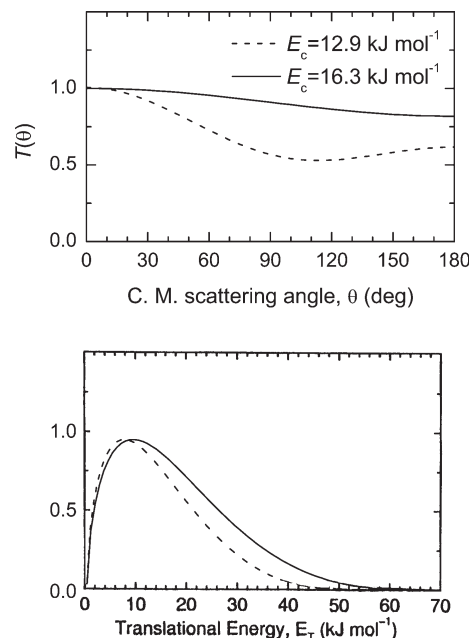


**Fig. 4** Best-fit center-of-mass translational energy (bottom) and angular flux (top) distributions for the reaction of atomic boron with acetylene at two collision energies.

collision energy, respectively. Finally, the relatively weak polarization of the angular distributions is likely the result of a little coupling between the initial  $L$  and final orbital angular momentum  $L'$ . For this specific mass combination, in fact, angular momentum partitioning arguments predict very high product rotational excitation, as a consequence of the much smaller reduced mass of the products,  $\mu'$ , with respect to that of the reagents,  $\mu$ . We recall that the magnitude of the final orbital angular momentum  $L'$  is given by  $\mu'v_r'b'$  while that of  $L$  is given by  $\mu v_r b$ , where  $v_r'$  and  $v_r$  are the relative velocities of products and reagents and  $b'$  and  $b$  are the final and initial impact parameters. For this reaction  $v_r$  and  $v_r'$  and  $b$  and  $b'$  are not expected to differ significantly. Therefore if  $\mu' \ll \mu$ ,  $L' \ll L$  and the final rotational angular momentum  $J'$  is about equal to  $L$  that is most of the total angular momentum is taken away from the rotation of the molecules and  $L$  and  $L'$  are weakly correlated. In this case the recoil velocity vector  $v'$  emerges out of the collision plane and the polarization at the poles is lost.<sup>30</sup>

## V. Discussion

In case of complex, polyatomic reactions it is often useful to combine the experimental data and the derived center-of-mass functions with electronic structure calculations. These investigations provide guidance, if, for instance, experimental enthalpies of formation of products are missing. In the present studies of the reaction of atomic boron with acetylene, the identification of the boron *versus* hydrogen exchange pathway strongly suggests the formation of the molecule with gross formula  $\text{C}_2\text{BH}$ . The experimentally determined exoergicity of  $31 \pm 10 \text{ kJ mol}^{-1}$  indicates further the synthesis of the linear  $\text{HBCC}(\text{X}^1\Sigma^+)$  isomer. A previous theoretical treatment yielded a reaction exoergicity of  $18 \pm 5 \text{ kJ mol}^{-1}$  close to the lower limit of our data.<sup>21</sup> Note that in the present situation, the best fit center-of-mass functions are very insensitive towards the high energy cutoff of the  $P(E_T)$ s, and no significant deviation in the fits has been observed by reducing the high energy cut-off by  $10\text{--}20 \text{ kJ mol}^{-1}$ . However, since the next stable structure is the linear  $\text{HCCB}(\text{X}^1\Sigma^+)$  isomer<sup>21</sup> and the channel leading to this isomer has been found to be endoergic by  $22 \pm 3 \text{ kJ mol}^{-1}$ , this isomer cannot be formed at the collision

energies ( $12.9 \text{ kJ mol}^{-1}$  and  $16.3 \text{ kJ mol}^{-1}$ ) of the present experiment.

Having assigned the reaction product as the  $\text{HBCC}(\text{X } ^1\Sigma^+)$  isomer, we attempt now to unravel the underlying dynamics. To this purpose, the collision energy dependence of the center-of-mass angular distributions provides important information. First, the significant intensity over the complete angular range suggests the presence of at least one channel which involves a  $\text{BC}_2\text{H}_2$  reaction intermediate and hence indirect dynamics (Fig. 4). Secondly, the forward scattered distributions suggest that at least one channel involves an incorporated boron atom and the leaving hydrogen atom located on opposite sides of the rotation axis of the fragmenting  $\text{BC}_2\text{H}_2$  intermediate. Combining these requirements with previous *ab initio* calculations on the doublet  $\text{BC}_2\text{H}_2$  surface helps us to eliminate potential intermediates (Fig. 5). Intrinsic reaction coordinate calculations showed that only the isomers **3**, **4**, and **5** connect to the  $\text{HBCC}(\text{X } ^1\Sigma^+) + \text{H}(^2\text{S}_{1/2})$  products. Among them, **5** can be ruled out to account at least for the forward-scattered microchannel. Recall that the reaction product is linear and hence can be excited only to *B*-like rotations, which give a rotational angular momentum  $j'$ . Since both reagents are prepared in a supersonic expansion, the initial rotational angular momentum  $j$  is much less than the initial orbital angular momentum  $L$ , and  $L \approx L' + j'$ . Here,  $L'$  denotes the final orbital angular momentum of the products. Due to the experimental relatively weak polarization of the center-of-mass angular distributions, we can conclude that  $L' \ll J$ , and, hence,  $L \approx j'$ . Therefore, most of the initial orbital angular momentum channels into *B*-like rotational excitations of the linear  $\text{HBCC}(\text{X } ^1\Sigma^+)$  product. To account for angular momentum conservation,  $j'$  must be parallel to the total angular momentum vector  $J$ , and the  $\text{HBCC}$  molecule likely rotates inside the molecular plane of the decomposing complex. Fig. 6 shows the principal axes of the intermediates **2**–**5**. In **5**, both hydrogen atoms are connected to the boron atom, and, hence, are located on the same side of the rotation axis as the incorporated  $\text{B}(^2\text{P}_j)$  atom. Therefore, an elimination of atomic hydrogen from **5** cannot account for the forward scattered

microchannel. Note that **5** can be only formed from **4** via ring opening through a transition state located  $90.5 \text{ kJ mol}^{-1}$  below the separated reactants. However, in the limit of a complete energy randomization, the calculated rate constant  $k_{4/5}$  is about 45 times smaller than  $k_{4/3}$ . This may suggest that the cyclic intermediate **4** rearrange to **3** rather than isomerizing to **5** (see Table 1). However, based on the calculated rate constants, most of **3** will go back to **4**, and a dynamic equilibrium will take place between **3** and **4** in favor of **3**, since the ratio  $k_{4/3}/k_{3/4}$  is about 4. **6** can then be formed from both **3** and **4**. Our calculations suggest that in the limit of a complete energy randomization about 20% of the reaction product will come from **4**, and 80% from **3**; the rate constant  $k_{3/6}$  is estimated to be of the same order of magnitude as  $k_{4/6}$ . The involvement of intermediate **4** is supported also by the experimentally found off-zero peaking of the center-of-mass translational energy distributions, as the fragmentation of intermediate **4** involves an exit barrier of  $12.6 \text{ kJ mol}^{-1}$ . This order-of-magnitude is similar as derived from the distribution maxima of both  $P(E_T)$ s between  $10$ – $15 \text{ kJ mol}^{-1}$ . Note that in the fragmenting intermediate **4**, the incorporated boron and the leaving hydrogen atom are located on opposite sides of the rotational axis and, hence, satisfy the experimental observation of forward-scattered center-of-mass angular distributions. The decomposing intermediate **4** can be formed *via* H migration in **2** through a bicyclic structure **2'**.

Based on these considerations, the following dynamics can be proposed. The boron atom adds barrier-less to the acetylene molecule forming **2**. This cyclic intermediate undergoes hydrogen migration to yield a weakly bound bicyclic intermediate **2'**, which itself rearranges to **4**. The latter rotates in a plane almost perpendicular to the total angular momentum vector and mostly isomerizes to **3**, which dissociates then to  $\text{HBCC}(\text{X } ^1\Sigma^+) + \text{H}(^2\text{S}_{1/2})$ . In the limit of RRKM calculations, about 20% of the products will come from **4**. The calculated lifetime of **4** of about 0.5 ps also supports the existence of a bound reaction intermediate and hence a theoretical confirmation of the experimentally found indirect reaction dynamics. We try to address now the remaining question, why an increased

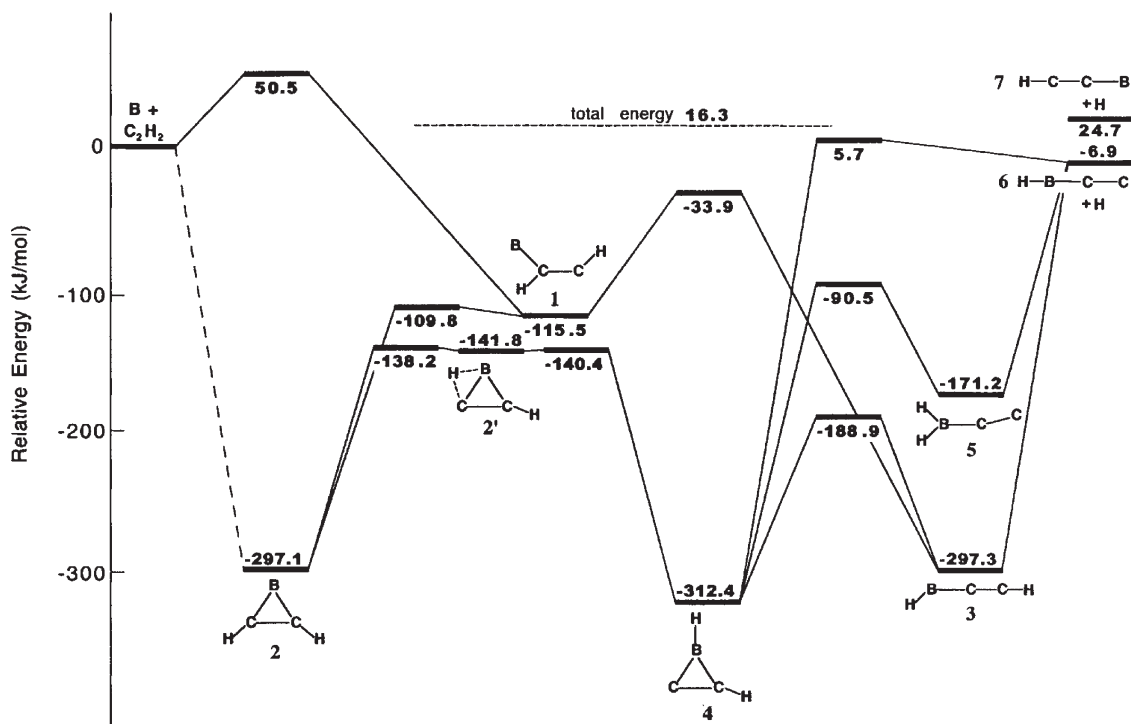
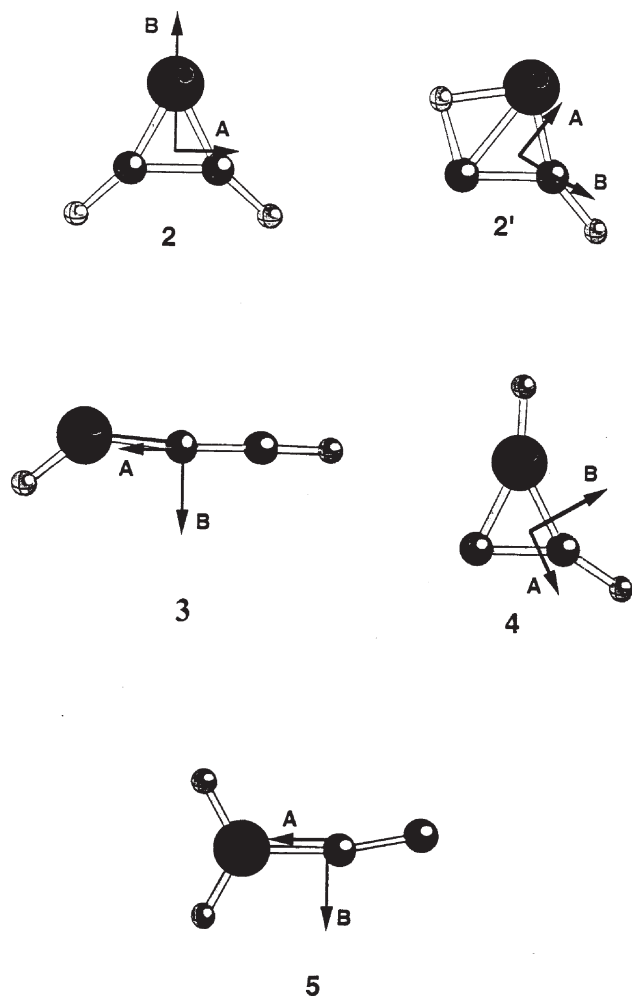


Fig. 5 Schematic representation of the  $\text{BC}_2\text{H}_2$  potential energy surface adapted from ref. 21. Only pathways involving the formation of the  $\text{HBCC}$  isomer are shown.



**Fig. 6** Schematic representation of the rotational axes of important reaction intermediates. The *C* axes are located perpendicular to the paper plane. The rotational constants *A*, *B*, and *C* (in GHz) are, respectively, 32.61997, 32.24908, 16.21673 (2), 34.34634, 29.33564, 15.82193 (2'), 1165.00072, 9.59148, 9.51316 (3), 40.00282, 25.52954, 15.58396 (4), and 213.72171, 9.77945, 9.35154 (5).

collision energy results into a less forward-peaked  $T(\theta)$ . Usually, rising the collision energy would result in an increase of  $I(0^\circ)/I(180^\circ)$ ,<sup>31</sup> under the most favorable reaction conditions, transitions from long-lived to oscillating complexes can be observed, and the life-time of the fragmenting intermediate can be estimated utilizing the intensity ratios at both poles of the  $T(\theta)$ . The reversed trend, however, is rather indicative of multiple, impact parameter-dependent microchannels, which can lead to the same reaction product. This has been observed experimentally in the crossed beams reaction of, for example, atomic carbon,  $C(^3P_j)$ , with ethylene.<sup>32</sup> Within the framework of the simple capture theory and the theoretically found barrier-less addition of atomic boron to form the intermediate 2, increasing the collision energy translates into a reduction of the maximum impact parameter.<sup>33</sup> As the collision energy rises, reactive trajectories with larger impact parameters, which can account for the forward peaking, are quenched.

Besides the experimentally observed observation of the HBCC( $X^1\Sigma^+$ ) isomer, we also investigated alternative exit channels theoretically. Table 2 reports the G2 calculated reaction energies.<sup>34</sup> G2 presents a composite method that corresponds effectively to calculations at the QCISD(T)/6-311+G(3df,2p) level on MP2(full)/6-31G(d) optimized geometries, incorporating scaled (by 0.8929) HF/6-31G(d) zero-point energies (ZPE) and a higher-level correction (HLC) term. The HLC is an empirical correction designed to compensate

**Table 2** Energetics of alternative exit channels in the reaction of atomic boron with acetylene

Reaction products	Reaction energy/kJ mol <sup>-1</sup>
HBCH( $X^2\Pi$ ) + C( $^3P_j$ )	+337
C <sub>2</sub> H( $X^2\Sigma^+$ ) + BH( $X^1\Sigma^+$ )	+212
CH <sub>2</sub> ( $X^3B_1$ ) + BC( $X^4\Sigma^-$ )	+459
HCB( $X^3\Pi$ ) + CH( $X^2\Pi_\alpha$ )	+457
BH <sub>2</sub> ( $X^2A_1$ ) + C <sub>2</sub> ( $X^1\Sigma_g^+$ )	+346
BC <sub>2</sub> ( $X^2A_1$ ) + H <sub>2</sub> ( $X^1\Sigma_g^+$ )	-14

for incomplete basis sets and other deficiencies in the theoretical treatment. G2 method has proved to be an accurate and efficient procedure for the prediction of molecular thermochemistry.<sup>35,36</sup> It is found that all these pathways except the one leading to H<sub>2</sub> and BC<sub>2</sub> are highly endoergic; therefore, these channels are closed within our experiment. The reaction leading to H<sub>2</sub> + BC<sub>2</sub> is calculated to be about 14 kJ mol<sup>-1</sup> exoergic. However, the lowest transition structure leading to these species is calculated to be 65 kJ mol<sup>-1</sup> higher than the separated boron and acetylene reactants.<sup>37</sup> This leads to the conclusions that the molecular hydrogen elimination pathway is also closed; hence—as verified experimentally—only the HBCC species can be formed under our experimental conditions.

## VI. Conclusions

The reaction of boron atoms, B( $^2P$ ), with acetylene, C<sub>2</sub>H<sub>2</sub>( $X^1\Sigma_g^+$ ), was investigated at two collision energies at the most fundamental microscopic level employing the crossed molecular beams technique. Forward-convolution fitting of the laboratory data at  $m/z = 36$  <sup>11</sup>BC<sub>2</sub>H<sup>+</sup> shows that only the boron *versus* atomic hydrogen exchange channel is open. The reaction dynamics are suggested to be indirect, proceed *via* addition of the boron atom to the carbon-carbon triple bond *via* a cyclic intermediate, and form—after successive isomerization—the linear HBCC( $X^1\Sigma^+$ ) isomer which is excited to *B*-like rotations. The formation of the HBCC( $X^1\Sigma^+$ ) structure under single collision conditions employing the crossed beams technique represents a first “clean”, gas phase synthesis following previous characterization in an argon matrix<sup>15</sup> and opens the way to a possible spectroscopic detection in the gas phase. Our results are in excellent agreement with recent matrix isolation experiments since most of the important species involved in the reaction mechanism 2, 3, 4 and 6 have been characterized by infrared spectroscopy.<sup>15</sup>

## Acknowledgements

RIK and NB acknowledge Academia Sinica, ROC, for providing the experimental setup. Y. H. thanks IDRIS (CNRS) project No. 337 for computer facilities. This work was performed within the *International Astrophysics Network*.

## References

- J. Niu, K. Rao and P. Jena, *J. Chem. Phys.*, 1997, **107**, 132.
- E. Hernandez, P. Ordejón, I. Boustani, A. Rubio and J. A. Alonso, *J. Chem. Phys.*, 2000, **113**, 3814.
- S. H. Bauer, *Chem. Rev.*, 1996, **96**, 1907.
- S. Yuasa, T. Yoshida, M. Kawashima and H. Isoda, *Combust. Flame*, 1998, **113**, 380.
- P. Jonsson, S. G. Johansson and C. F. Fischer, *Astrophys. J.*, 1994, **429**, 45.
- L. E. Ennis and A. P. Hitchcock, *J. Chem. Phys.*, 1999, **111**, 3468.
- C. Olliver and P. Renaud, *Chem. Rev.*, 2001, **101**, 3415.

- 8 E. L. Dreizin, D. G. Keil, W. Felder and E. P. Vicenzi, *Combust. Flame*, 1999, **119**, 272.
- 9 R. O. Foelsche, R. L. Burton and H. Krier, *Combust. Flame*, 1999, **117**, 32.
- 10 M. J. Spalding, H. Krier and R. L. Burton, *Combust. Flame*, 2000, **120**, 200.
- 11 D. S. P. Dearborn, D. N. Schramm, G. Steigman and J. Truran, *Astrophys. J.*, 1989, **347**, 455.
- 12 K. Cunha, D. L. Lambert, M. Lemke, D. R. Gies and L. C. Roberts, *Astrophys. J.*, 1997, **478**, 211.
- 13 E. Casuso and J. E. Beckman, *Astrophys. J.*, 1997, **475**, 155.
- 14 J. C. Howk, K. R. Sembach and B. D. Savage, *Astrophys. J.*, 2000, **543**, 278.
- 15 L. Andrews, P. Hassanzadeh, J. M. L. Martin and P. R. Taylor, *J. Phys. Chem.*, 1993, **97**, 5839.
- 16 L. Andrews, D. V. Lanzisera, P. Hassanzadeh and Y. Hannachi, *J. Phys. Chem. A*, 1998, **102**, 3259.
- 17 J. M. L. Martin, P. R. Taylor, P. Hassanzadeh and L. Andrews, *J. Am. Chem. Soc.*, 1993, **115**, 2510.
- 18 N. Galland, Y. Hannachi, D. V. Lanzisera and L. Andrews, *Chem. Phys.*, 2000, **255**, 205.
- 19 N. Balucani, O. Asvany, Y. T. Lee, R. I. Kaiser, N. Galland and Y. Hannachi, *J. Am. Chem. Soc.*, 2000, **122**, 11 234.
- 20 R. I. Kaiser and H. F. Bettinger, *Angew. Chem. Int. Ed.*, 2002, **41**, 2350.
- 21 N. Balucani, O. Asvany, Y. T. Lee, R. I. Kaiser, N. Galland, M. T. Rayez and Y. Hannachi, *J. Comput. Chem.*, 2001, **22**, 1359.
- 22 M. E. Volpin, Yu. D. Koreshkov, V. G. Dulova and D. N. Kursanov, *Tetrahedron*, 1962, **18**, 107.
- 23 P. Casavecchia, *Rep. Prog. Phys.*, 2000, **63**, 355; Y. T. Lee, in *Atomic and Molecular Beam Methods*, ed. G. Scoles, Oxford University Press, New York, 1987, vol. 1, p. 553.
- 24 R. I. Kaiser and N. Balucani, *Acc. Chem. Res.*, 2001, **34**, 699.
- 25 N. Balucani, A. M. Mebel, Y. T. Lee and R. I. Kaiser, *J. Phys. Chem. A*, 2001, **105**, 9813; N. Balucani, L. Cartechini, M. Alagia, P. Casavecchia and G. G. Volpi, *J. Phys. Chem. A*, 2000, **104**, 5655; N. Balucani, M. Alagia, L. Cartechini, P. Casavecchia, G. G. Volpi, K. Sato, T. Takayanagi and Y. Kurosaki, *J. Am. Chem. Soc.*, 2000, **122**, 4443.
- 26 N. Balucani, O. Asvany, A. H. H. Chang, S. H. Lin, Y. T. Lee, R. I. Kaiser, H. F. Bettinger, P. v. R. Schleyer and H. F. Schaefer III, *J. Chem. Phys.*, 1999, **111**, 7457.
- 27 R. I. Kaiser, J. Ting, L. C. L. Huang, N. Balucani, O. Asvany, Y. T. Lee, H. Chan, D. Stranges and D. Gee, *Rev. Sci. Instrum.*, 1999, **70**, 4185.
- 28 H. Eyring, S. H. Lin and S. M. Lin, *Basic Chemical Kinetics*, Wiley, New York, 1980.
- 29 W. Forst, *Theory of Unimolecular Reaction*, Academic Press, New York, 1973.
- 30 R. I. Kaiser and A. M. Mebel, *Int. Rev. Phys. Chem.*, 2002, **21**, 307.
- 31 R. I. Kaiser, *Chem. Rev.*, 2002, **102**, 1309.
- 32 R. I. Kaiser, Y. T. Lee and A. G. Suits, *J. Chem. Phys.*, 1996, **105**, 8705.
- 33 R. D. Levine and R. B. Bernstein, *Molecular Reaction Dynamics and Chemical Reactivity*, Oxford University Press, Oxford, 1987.
- 34 L. A. Curtiss, K. Raghavachari, G. W. Trucks and J. A. Pople, *J. Chem. Phys.*, 1991, **94**, 7221.
- 35 L. A. Curtiss and K. Raghavachari, in *Quantum Mechanical Electronic Structure Calculations with Chemical Accuracy*, ed. S. R. Langhoff, Kluwer Academic, Netherlands, 1995.
- 36 K. Raghavachari and L. A. Curtiss, in *Modern Electronic Structure Theory*, ed. D. R. Yarkony, World Scientific, Singapore, 1995.
- 37 N. Galland, PhD Thesis, Université Bordeaux I, June 2002.